The New Fundamental Plane Dictating Galaxy Cluster Evolution

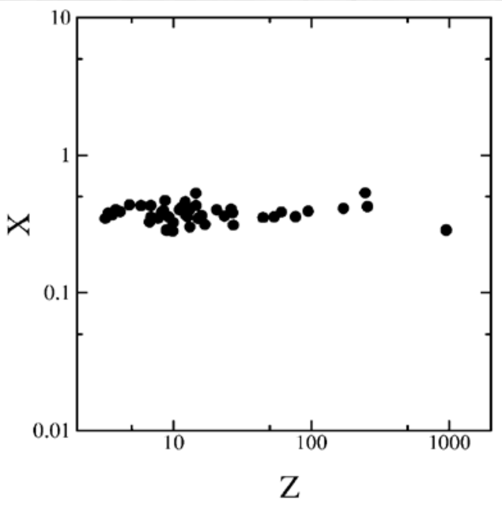

Fujita & Takahara (1999)
see also Ota et al. (2006)

Yutaka Fujita (Osaka, Japan)

Y. Fujita, K. Umetsu, E. Rasia, M. Meneghetti, M. Donahue, E. Medezinski, N. Okabe, & M. Postman, 2018, ApJ, 857, 118

Y. Fujita, K. Umetsu, S. Ettori, E. Rasia, N. Okabe, & M. Meneghetti, 2018, ApJ, 363, 37

Y. Fujita, S. Ettori, M. Donahue, K. Umetsu, E. Rasia, M. Meneghetti, E. Medezinski, N. Okabe, & M. Postman, submitted (Review)

Y. Fujita, H, Aung, & D. Nagai, in preparation

Contents

- Introduction
  - Structure and evolution of galaxy clusters
- Fundamental plane (FP) analysis
  - CLASH and X-ray cluster samples
- Numerical simulations
- Origin of the FP
  - Similarity solution of cluster formation
- Applications
  - Mass-temperature and luminosity-temperature relation of clusters
  - Mass calibration of clusters
- Summary

Structure of Clusters

- Clusters mainly composed of dark matter
- NFW density profile
  - Navarro, Frenk & White (1997)

$$\rho_{\mathrm{DM}}(r) = \frac{\delta_c \rho_c}{(r/r_s)(1+r/r_s)^2}$$

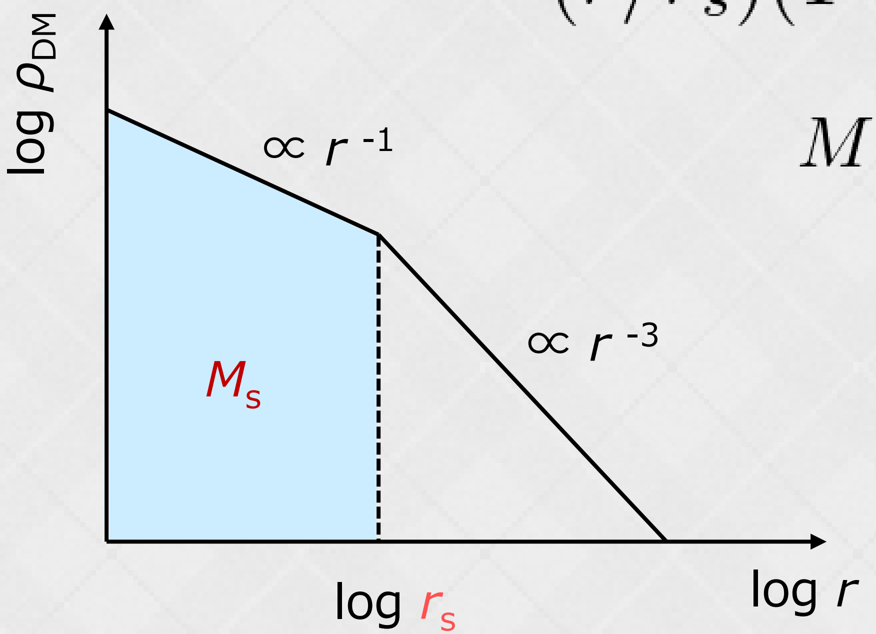

$$M(r) = \int_0^r 4\pi \rho_{\mathrm{DM}}(r) r^2 dr$$

$$M_s \equiv M(r_s)$$

Inside-out scenario

- Cluster internal structure reflects their growth history

1. Fast growth phase
   - Inner region ($r \lesssim r_s$) rapidly grows through massive matter accretion
2. Slow growth phase
   - Outskirts of clusters ($r \gtrsim r_s$) slowly grows through moderate matter accretion and the inner structure (r_s, M_s) is preserved during this phase
     - Wechsler et al. (2002), Zhao et al. (2003), Ludlow et al. (2013), Correa et al. (2015), More et al. (2015) (see also Salvador-Solé et al.1998; Fujita & Takahara 1999)

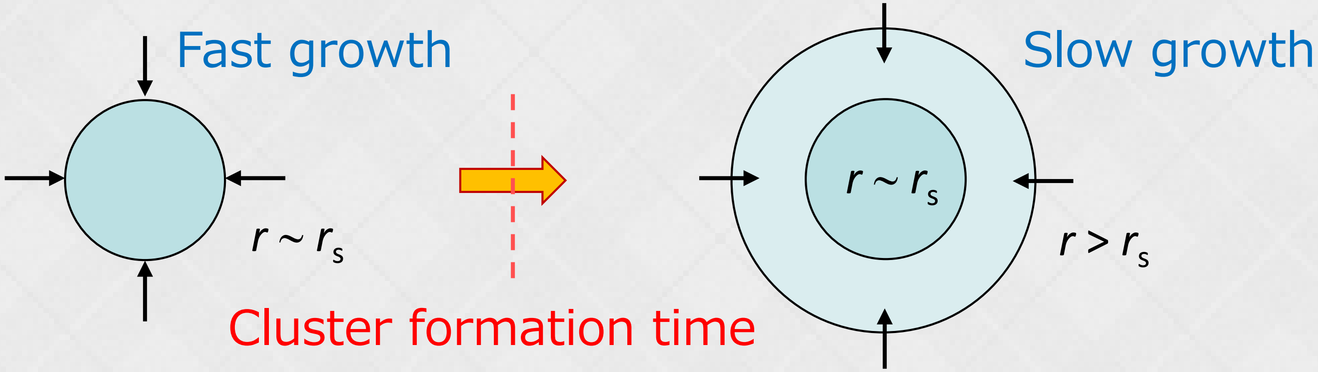

▶ Cluster age in the inside-out scenario

- Cluster formation time
  - Transition time from the fast to the slow growth phase
  - Older cluster have a larger characteristic density, $\rho_s = 3\, M_s/(4\pi\, r_s{}^3)$
    - The density depends on clusters
  - The density reflects that of the background Universe at the formation time
    - Clusters with larger ρ_s formed earlier
    - (r_s, M_s) or ρ_s does not much change after the formation
      - Navarro et al. (1997), Zhao et al. (2009), Ludlow et al. (2013), Correa et al. (2015)

Concentration Parameter

- $c_\Delta = r_s/r_\Delta$
  - $M_\Delta = M(< r_\Delta)$
  - $3\,M_\Delta/(4\pi\, r_\Delta{}^3) = \Delta\,\rho_c$
    - ρ_c: critical density of the Univ.
    - $\Delta = 200$ or 500 is often used
- c_Δ is a function of M_Δ, but has a large dispersion
  - Dispersion of cluster formation time
    - The more concentrated, the older the object is

c_Δ-M_Δ relation

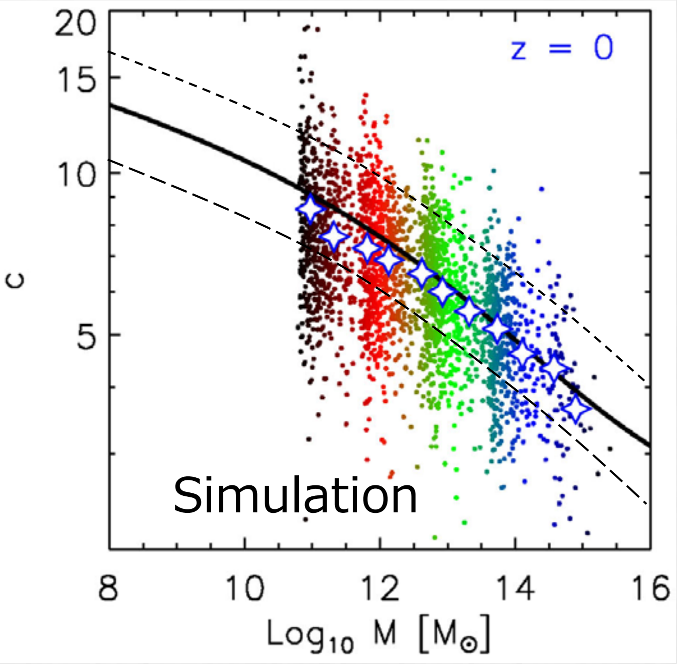

Correa et al. (2015)

▶ Inside-out scenario and ICM

- The Inside-out scenario has been studied mainly for simulated dark-matter halos
  - How about real (observed) objects?
  - How about intracluster medium (ICM)?
- We tried to systematically explain the growth of clusters based on the modern inside-out scenario by studying the combination of parameters (r_s, M_s, T_X)
  - T_X (X-ray temperature) mainly reflects X-ray emissions at $r \lesssim r_s$ and should be affected by the gravitational potential there

CLASH cluster sample

- 20 massive clusters
  - z = 0.187- 0.686
- r_s, M_s
  - Gravitational lensing (HST, Subaru)
    - Umetsu+16
- T_X (core excised)
  - Chandra observations
    - Donahue+14
- We study data distribution in the space of (log r_s, log M_s, log T_X)

Cluster	z	r_s (kpc)	r_{200} (kpc)	M_s ($10^{14}\,M_\odot$)	M_{200} ($10^{14}\,M_\odot$)	T_X (keV)
Abell 383	0.187	304^{+159}_{-97}	1800^{+209}_{-189}	$1.4^{+1.0}_{-0.5}$	$7.9^{+3.1}_{-2.2}$	6.5 ± 0.24
Abell 209	0.206	834^{+243}_{-192}	2238^{+161}_{-172}	$5.2^{+2.2}_{-1.6}$	$15.4^{+3.6}_{-3.3}$	7.3 ± 0.54
Abell 2261	0.224	682^{+232}_{-170}	2542^{+192}_{-188}	$5.8^{+2.7}_{-1.8}$	$22.9^{+5.6}_{-4.7}$	7.6 ± 0.30
RX J2129.7+0005	0.234	294^{+133}_{-89}	1626^{+163}_{-154}	$1.1^{+0.7}_{-0.4}$	$6.1^{+2.0}_{-1.6}$	5.8 ± 0.40
Abell 611	0.288	560^{+250}_{-172}	2189^{+204}_{-208}	$3.8^{+2.3}_{-1.5}$	$15.6^{+4.8}_{-4.0}$	7.9 ± 0.35
MS 2137-2353	0.313	784^{+557}_{-357}	2064^{+261}_{-286}	$4.7^{+5.2}_{-2.6}$	$13.4^{+5.8}_{-4.9}$	5.9 ± 0.30
RX J2248.7-4431	0.348	643^{+422}_{-246}	2267^{+282}_{-261}	$4.9^{+4.8}_{-2.3}$	$18.5^{+7.8}_{-5.7}$	12.4 ± 0.60
MACS J1115.9+0129	0.352	738^{+249}_{-196}	2186^{+161}_{-174}	$5.1^{+2.4}_{-1.7}$	$16.6^{+4.0}_{-3.7}$	8.0 ± 0.40
MACS J1931.8-2635	0.352	501^{+441}_{-221}	2114^{+355}_{-311}	$3.5^{+4.6}_{-1.8}$	$15.0^{+8.9}_{-5.7}$	6.7 ± 0.40
RX J1532.9+3021	0.363	293^{+433}_{-114}	1544^{+191}_{-210}	$1.2^{+1.6}_{-0.5}$	$5.9^{+2.5}_{-2.1}$	5.5 ± 0.40
MACS J1720.3+3536	0.391	505^{+248}_{-162}	2055^{+204}_{-204}	$3.4^{+2.3}_{-1.4}$	$14.4^{+4.7}_{-3.9}$	6.6 ± 0.40
MACS J0416.1-2403	0.396	642^{+201}_{-156}	1860^{+146}_{-154}	$3.4^{+1.5}_{-1.1}$	$10.7^{+2.7}_{-2.4}$	7.5 ± 0.80
MACS J0429.6-0253	0.399	394^{+238}_{-143}	1792^{+225}_{-208}	$2.1^{+1.8}_{-0.9}$	$9.6^{+4.1}_{-3.0}$	6.0 ± 0.44
MACS J1206.2-0847	0.440	587^{+248}_{-176}	2181^{+165}_{-178}	$4.6^{+2.4}_{-1.7}$	$18.1^{+4.4}_{-4.1}$	10.8 ± 0.60
MACS J0329.7-0211	0.450	254^{+95}_{-63}	1697^{+129}_{-127}	$1.4^{+0.6}_{-0.4}$	$8.6^{+2.1}_{-1.8}$	8.0 ± 0.50
RX J1347.5-1145	0.451	840^{+339}_{-239}	2684^{+226}_{-230}	$9.8^{+5.6}_{-3.6}$	$34.2^{+9.4}_{-8.1}$	15.5 ± 0.60
MACS J1149.5+2223	0.544	1108^{+404}_{-291}	2334^{+169}_{-178}	$10.8^{+5.4}_{-3.7}$	$25.0^{+5.8}_{-5.3}$	8.7 ± 0.90
MACS J0717.5+3745	0.548	1300^{+347}_{-271}	2387^{+154}_{-165}	$13.2^{+5.3}_{-3.9}$	$26.8^{+5.6}_{-5.2}$	12.5 ± 0.70
MACS J0647.7+7015	0.584	468^{+254}_{-160}	1884^{+189}_{-192}	$3.3^{+2.3}_{-1.3}$	$13.7^{+4.6}_{-3.8}$	13.3 ± 1.80
MACS J0744.9+3927	0.686	574^{+269}_{-192}	1982^{+179}_{-185}	$4.9^{+3.1}_{-2.0}$	$17.9^{+5.3}_{-4.6}$	8.9 ± 0.80

YF, Umetsu, Rasia, Meneghetti, Donahue, Medezinski, Okabe, & Postman (2018)

▶ Fundamental plane (FP) analysis

- For CLASH clusters
- Data points form a thin plane (FP)
  - T_X is strongly correlated to (r_s, M_s)
    - T_X is also determined by the cluster formation time
  - X-ray sample (Ettori+10) also forms the FP

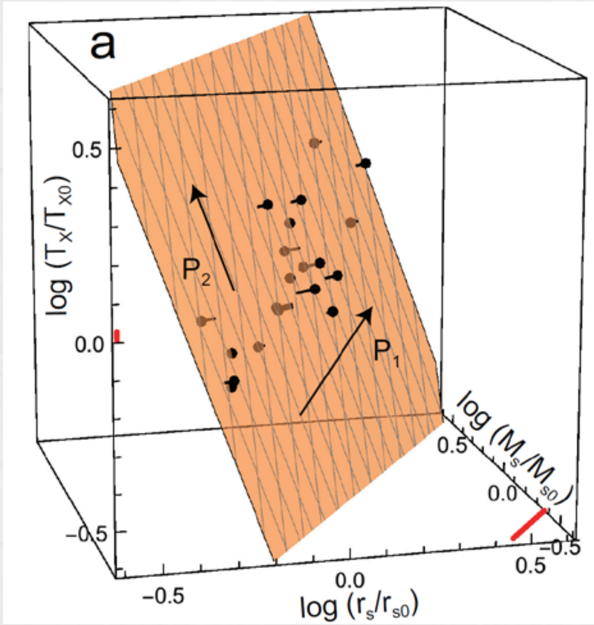

Cross-section

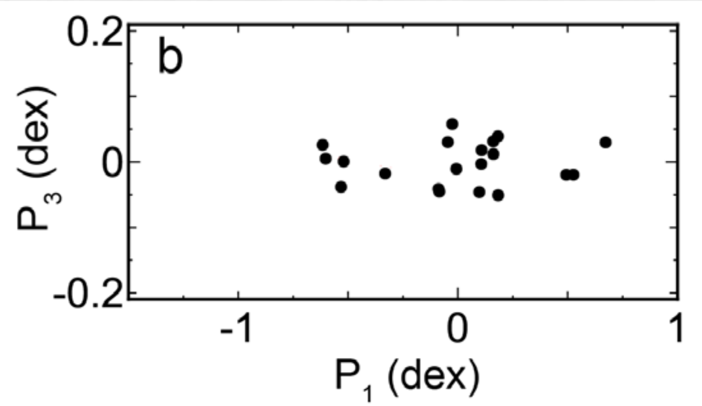

Fujita et al. (2018a)

Plane angle

- Direction of the plane normal P_3
  - The angle is inconsistent with simplified “virial equilibrium”, $T_X \propto M_s/r_s$

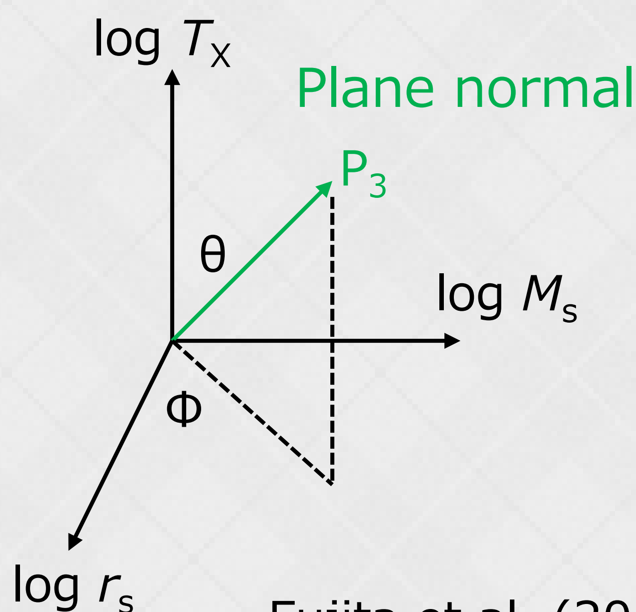

Fujita et al. (2018a)

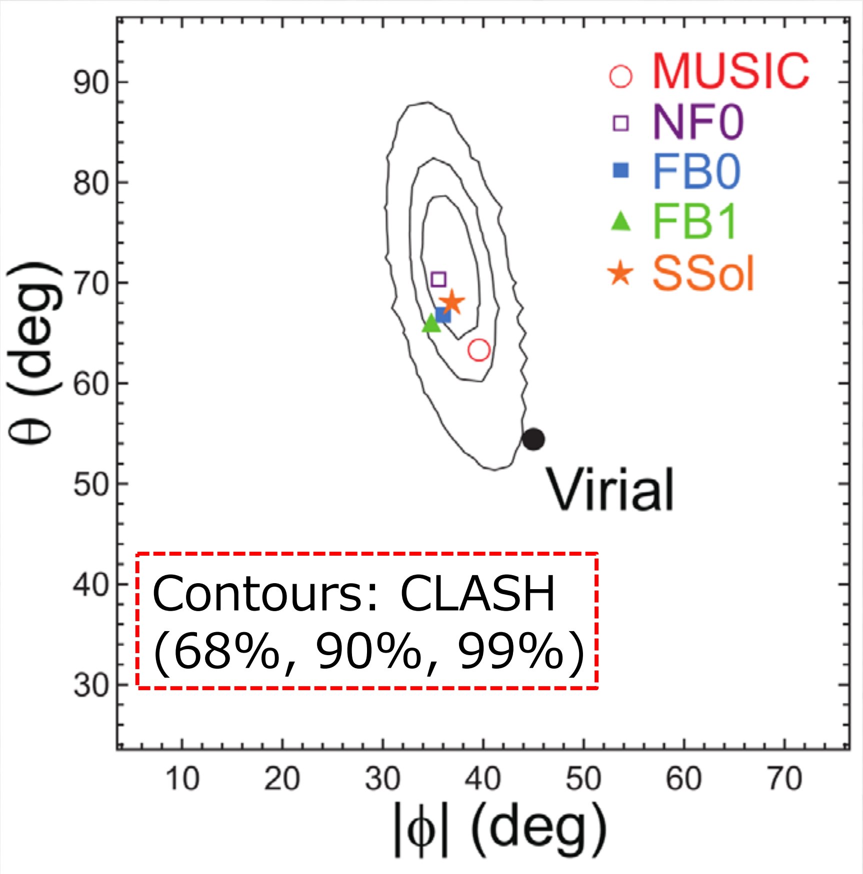

▶ Numerical simulations

- Radiative cooling + feedback simulations (FB0, FB1) by Rasia et al. (2015)
  - FB1 (z = 1) and FB0 (z = 0) points are on the same plane
    - Clusters evolve along the plane in the direction of P_1 (major axis)
  - The angle is consistent with that of the CLASH
  - FB0 plane is almost same as NF0 (adiabatic) plane
    - The effects of cooling and feedback are ignorable at $r \sim r_s$ > core radius

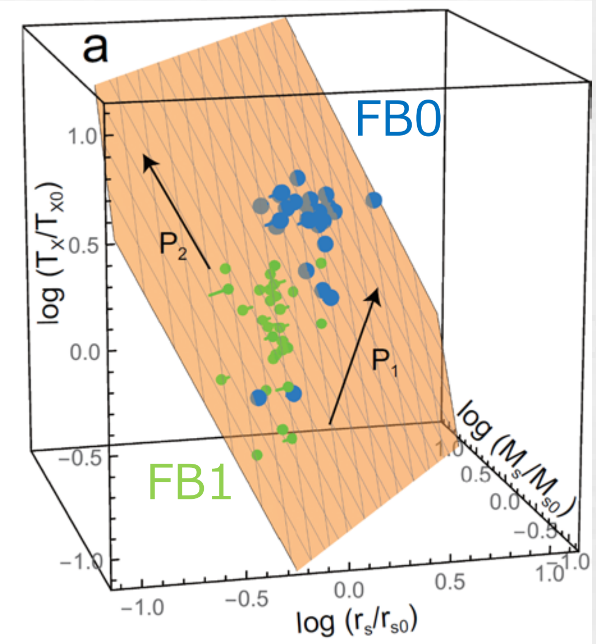

Cross-section

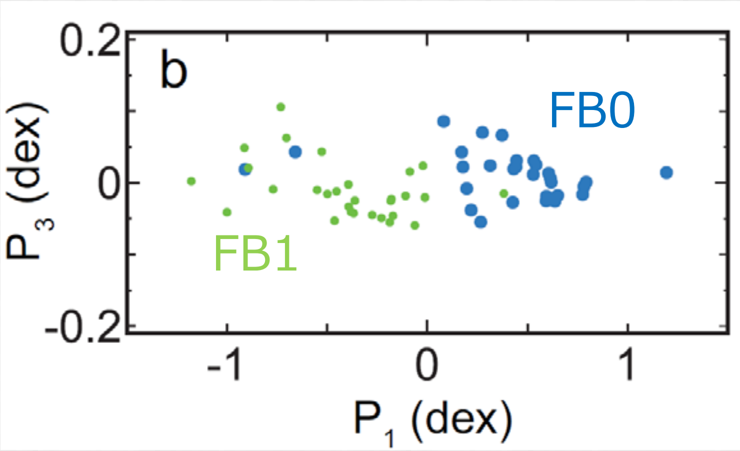

Fujita et al. (2018a)

Details of cluster evolution

- Clusters move along P_1 ($r_s \propto M_s^{1/2}$)
- Even during major mergers (A, B, E), clusters do not much deviate from the FP
  - T_X and r_s, M_s are anti-correlated
  - Contribute to the thinness of the FP

Evolution of a cluster

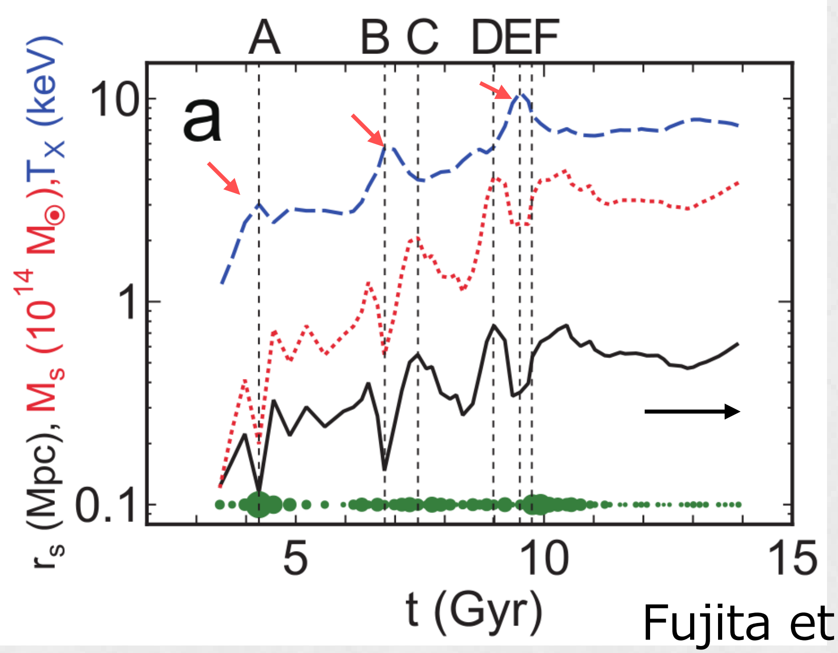

Evolution of a cluster on the FP

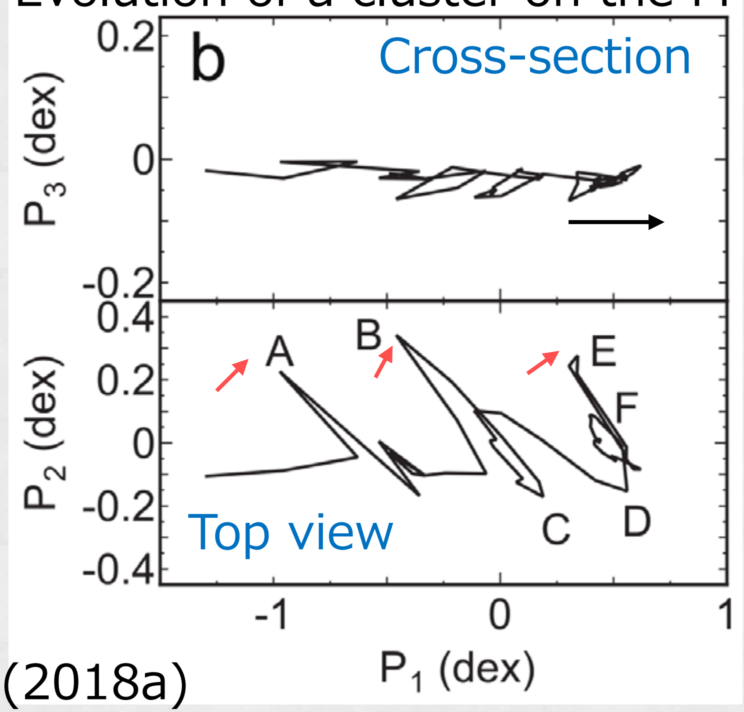

Fujita et al. (2018a)

Cluster merger

- T_X and r_s, M_s are anti-correlated

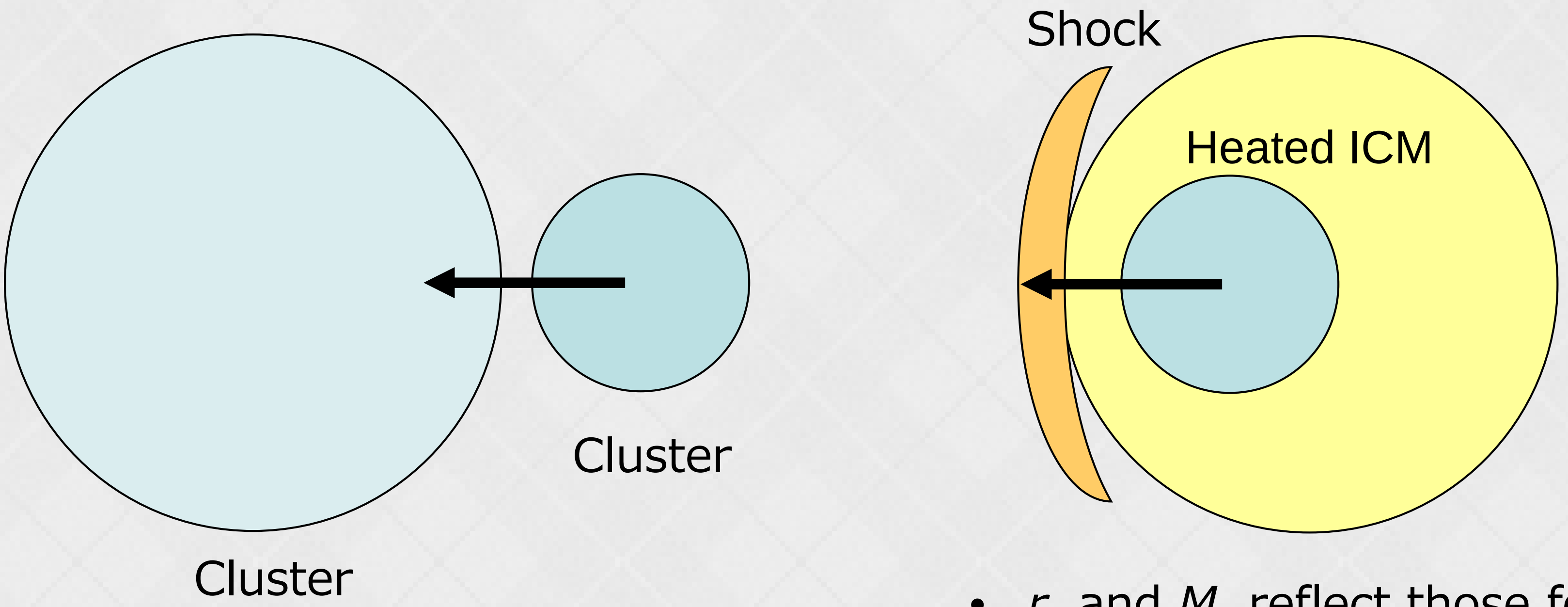

- r_s and M_s reflect those for the smaller cluster
- T_X increases

Similarity solution

- What makes the strange angle of the plane?
- We attempted to explain it using the similarity solution by Bertschinger (1985)
  - Secondary infall and accretion onto an initially overdense perturbation

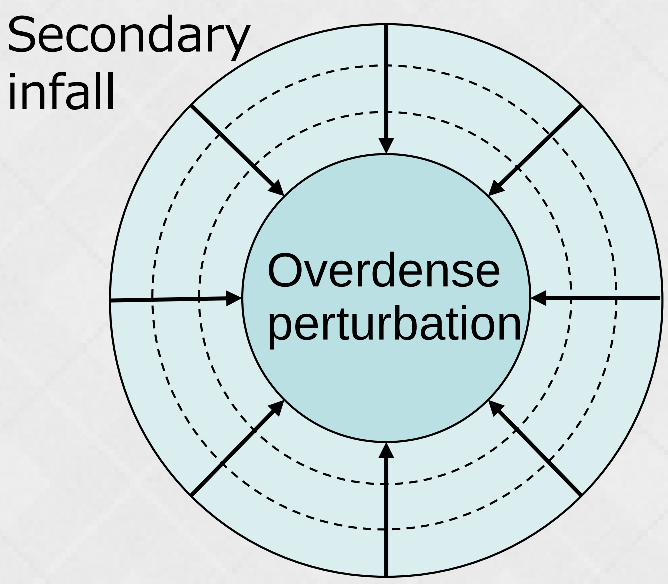

V: velocity
D: density
P: pressure
M: mass
λ: radius

Nondimensional profiles

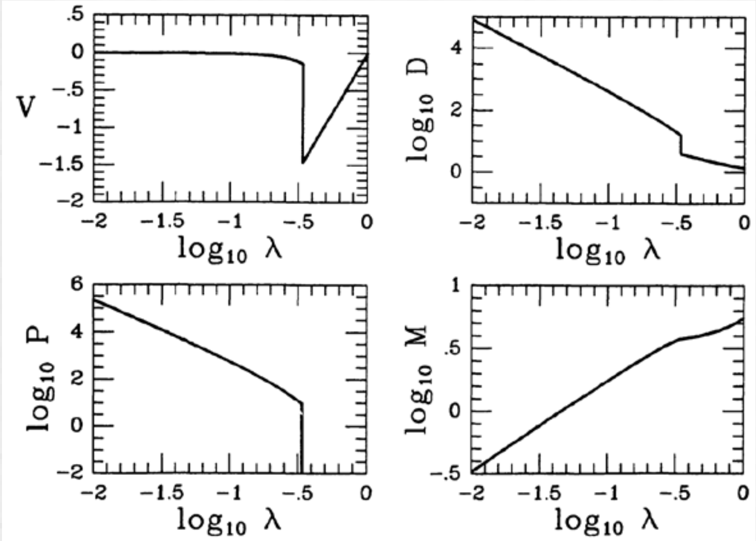

Bertschinger (1985)

Similarity solution and FP

- The similarity solution has an entropy integral

$$P(\lambda)D(\lambda)^{-\gamma}M(\lambda)^{10/3-3\gamma} = \mathrm{const} \qquad (\gamma = 5/3)$$

  - Nondimensional parameters
    - P: pressure, D: density
    - M: mass, λ: radius

$$\Rightarrow \quad r_s^2 M_s^{-3/2} T_X = \mathrm{const}$$

      - Relation among dimensional parameters

  - The angle of the plane (SSol) is consistent with observations and simulations

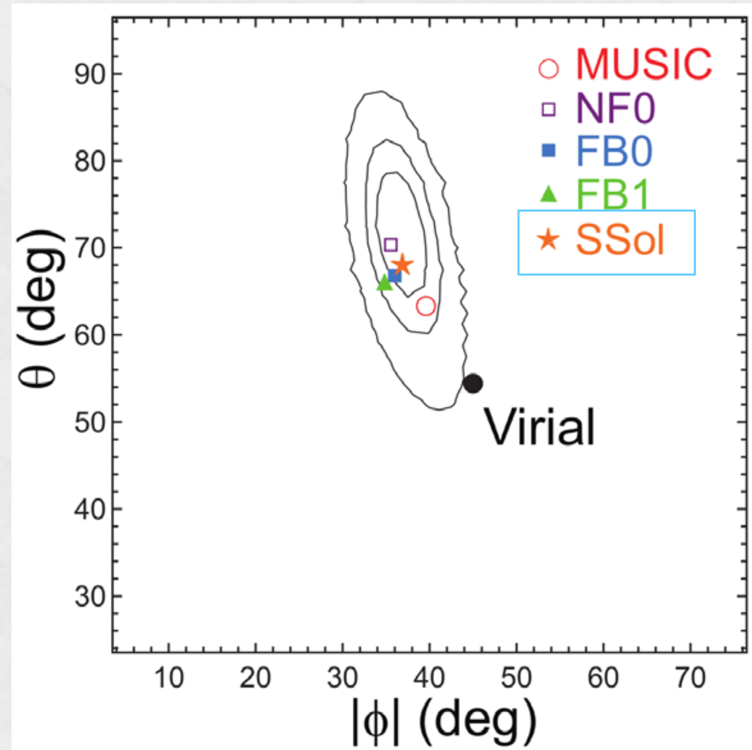

Fujita et al. (2018a)

Similarity sol. vs. conventional model

- Conventional spherical collapse model

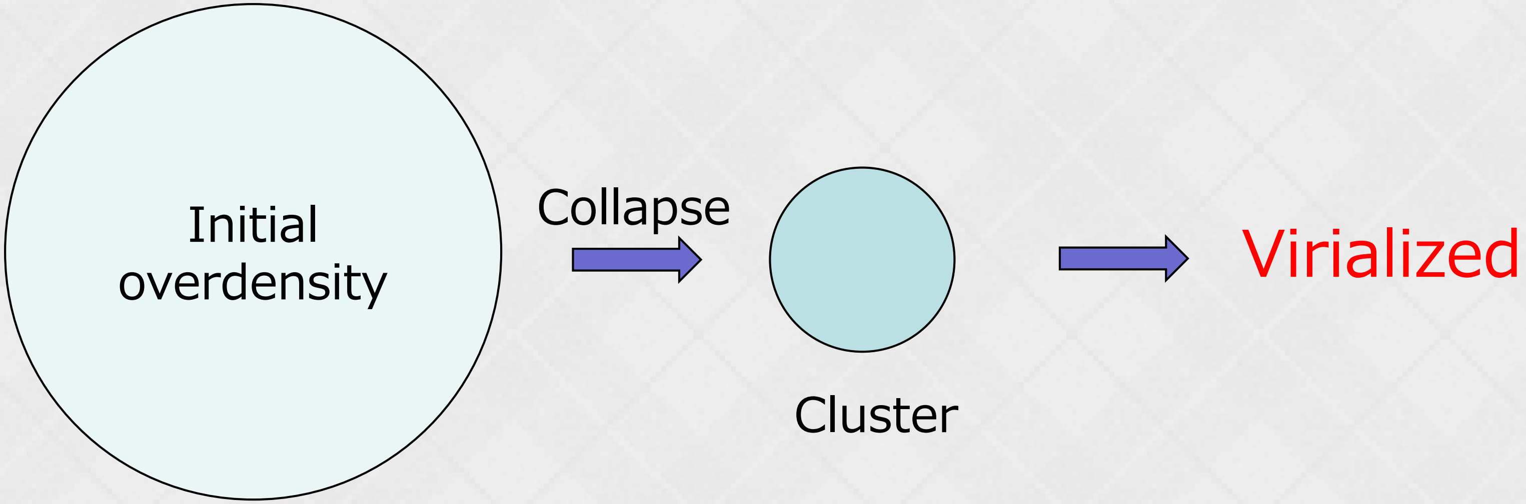

  - It is implicitly assumed that the universe is empty outside the cluster
    - It is not true

▶ Similarity sol. vs. conventional model

- Similarity solution (Bertschinger 1985)

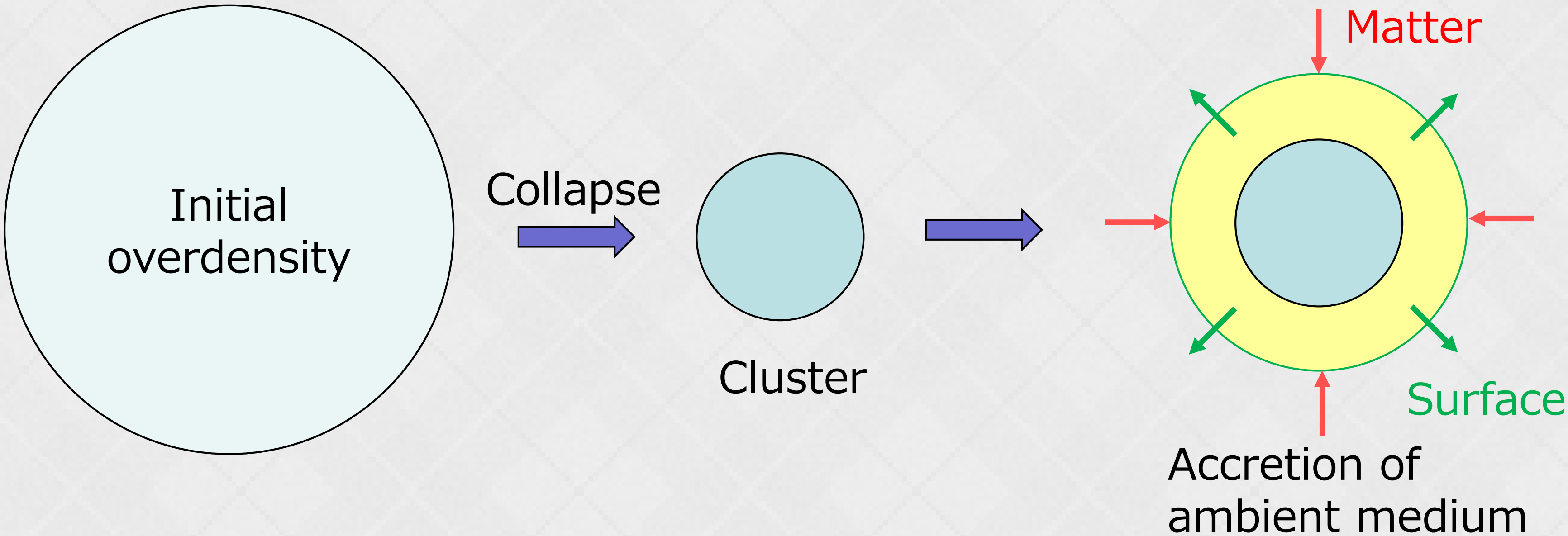

- More realistic than the conventional model
  - The mass and size continue to increase
  - The surface of clusters is affected by the flux of inertia and pressure of infalling materials

Virial theorem

- Virial equilibrium

  0 = 2 (kinetic/thermal energy) + (potential energy)

- Virial theorem

  (Change of mass and volume)
  = 2 (kinetic/thermal energy) + (potential energy)
  + (surface term)

  - Our results indicate that the two green terms cannot be ignored

- Note that hydrostatic equilibrium is well established in the similarity solution

Cluster motion on the FP

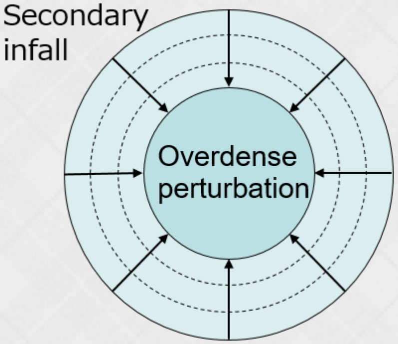

- From a scaling relation (Kaiser 1986)

$$r_s \propto M_s^{1/2}$$

  - Overdense perturbation follows the initial density fluctuations of the universe.

- This direction is the same as P_1 or the direction of cluster evolution shown by simulations
  - Cluster evolution follows the spectrum of the initial density fluctuations of the Universe

FP projected on r_s-M_s

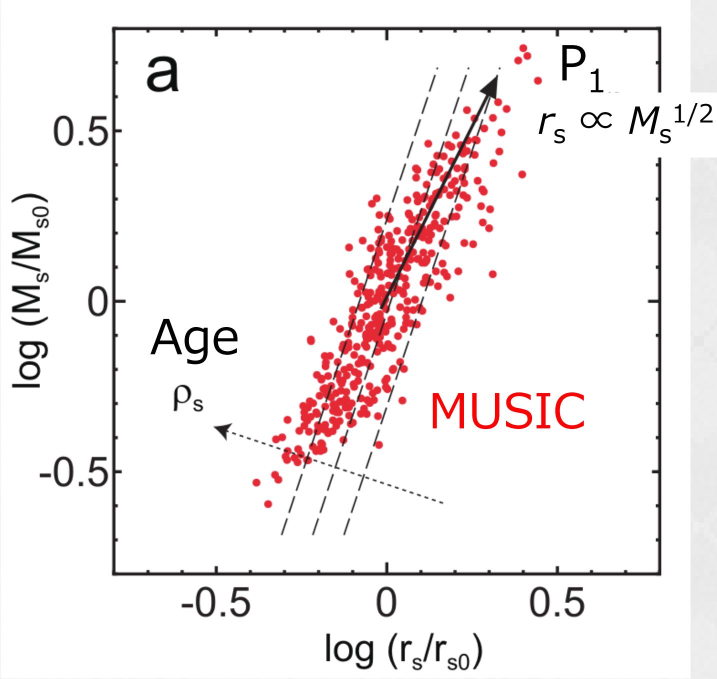

Fujita et al. (2018a)

▶ Dispersion of $c-M$ relation

- $c_\Delta(M_\Delta,z)$-M_Δ relation can be converted to M_s-r_s relation (black lines)
- The dispersion of the $c_\Delta(M_\Delta, z)$-M_Δ relation (dotted and dashed lines) corresponds to the distribution of clusters on the FP and the cluster age

FP projected on r_s-M_s plane

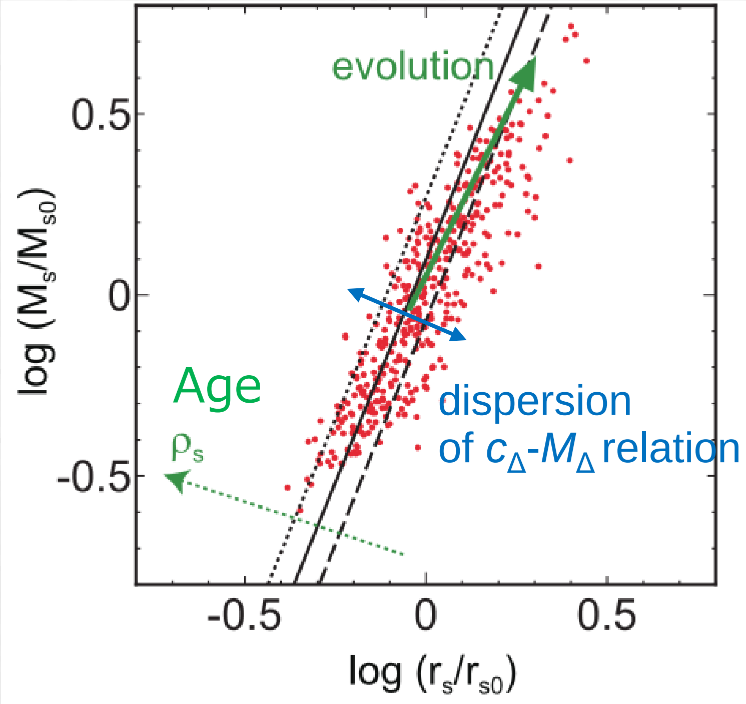

Red dots: MUSIC simulation

▶ Applications of the FP

- Mass-temperature (*M*-*T*) relation
  - $M_\Delta \propto T_X^{3/2}$ is a good approximation
    - $M_\Delta = M(< r_\Delta)$
    - $3\,M_\Delta/(4\pi\, r_\Delta^{\,3}) = \Delta\,\rho_c$
      - ρ_c: critical density of the Univ.
      - $\Delta = 200$ or 500 is often used

Simulation + Observation

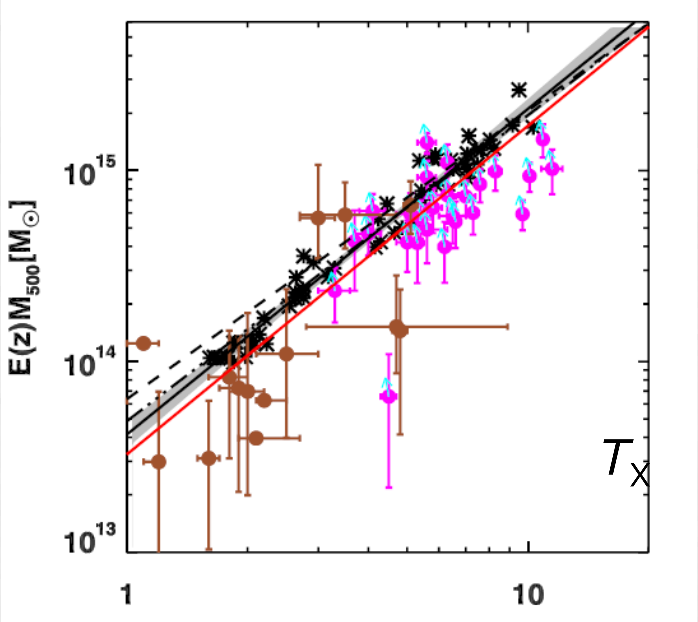

Truong et al. (2018)

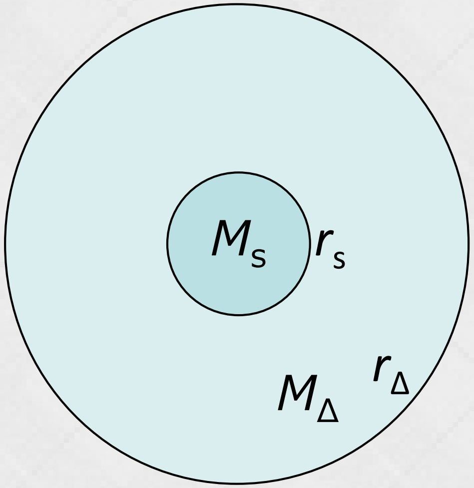

$r_\Delta > r_s$

Δ = 200 or 500

▶ Conventional explanation

- Assumptions
  - Clusters are well-virialized and isothermal within r_Δ
  - Representative density of clusters is $\rho_\Delta \equiv \Delta\, \rho_c$ (not ρ_s)
  - T_X is primarily determined on a scale of r_Δ (not r_s)
- Mass and temperature

$$M_\Delta = 4\pi\rho_\Delta r_\Delta^3/3$$
$$T_X \propto M_\Delta/r_\Delta \propto \rho_\Delta r_\Delta^2 \propto r_\Delta^2 \quad \Rightarrow \quad M_\Delta \propto T_X^{3/2}$$

- However, the assumptions are inconsistent with the "inside-out" scenario
  - The region $r < r_s$ keeps the cluster's old memory
    - Clusters are not well-relaxed (virialized)
      - NFW profile is not an isothermal profile

New interpretation

- Fundamental plane

$$T_X = T_{X0} \left(\frac{r_s}{r_{s0}} \right)^{-2} \left(\frac{M_s}{M_{s0}} \right)^{(n+11)/6}$$

n: index of initial density fluctuations

- Concentration parameter

$$c_\Delta(M_\Delta, z) = r_\Delta / r_s$$

  - The mass dependence can be explained by the inside-out scenario
  - We use an analytical form
    - Duffy et al. (2008), Bhattacharya et al. (2013), Dutton & Maccio (2014), Meneghetti et al. (2014), Diemer & Kravtsov (2015)

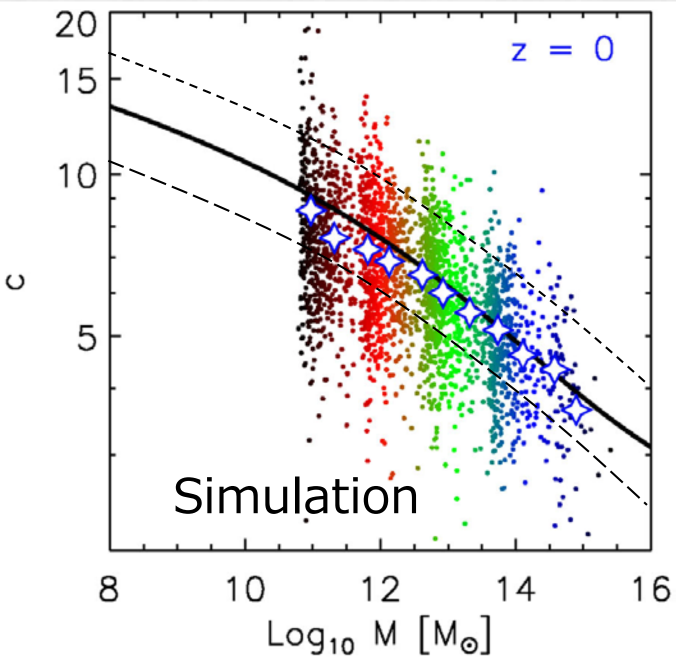

Correa et al. (2015)

▶ *M* – *T* relation

- r_s, M_s are functions of M_Δ and $c_\Delta(M_\Delta, z)$
- M_Δ -T_X relation is derived from the FP relation,

$$T_X = T_{X0}\left(\frac{r_s}{r_{s0}}\right)^{-2}\left(\frac{M_s}{M_{s0}}\right)^{(n+11)/6}$$

- $M_\Delta \propto T_X^{3/2}$ is well reproduced
  - Virial assumption is not used
  - The dispersion is caused by that of $c_\Delta(M_\Delta,z)$-M_Δ

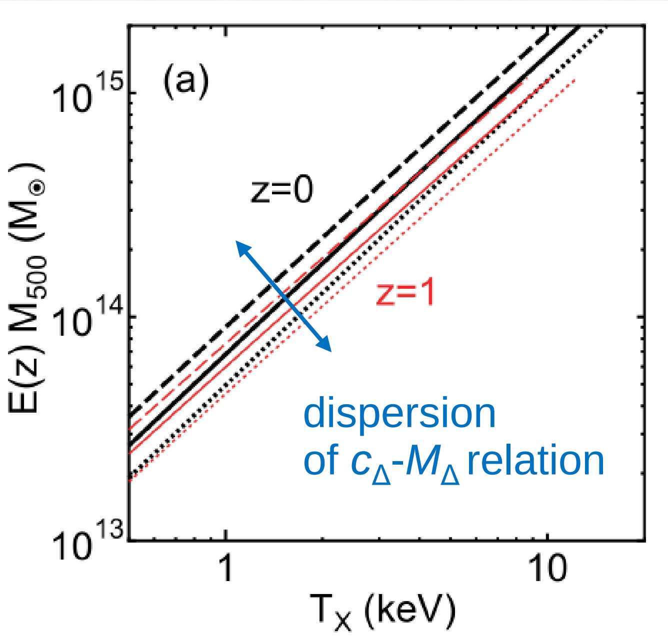

YF, Umetsu, Ettori, Rasia, Okabe, & Meneghetti (2018)

FP for mass calibration

- FP for the X-ray sample (Ettori+ 10, XFP)
- FP for the CLASH sample (CFP)
  - Their positions are slightly different

Cross section

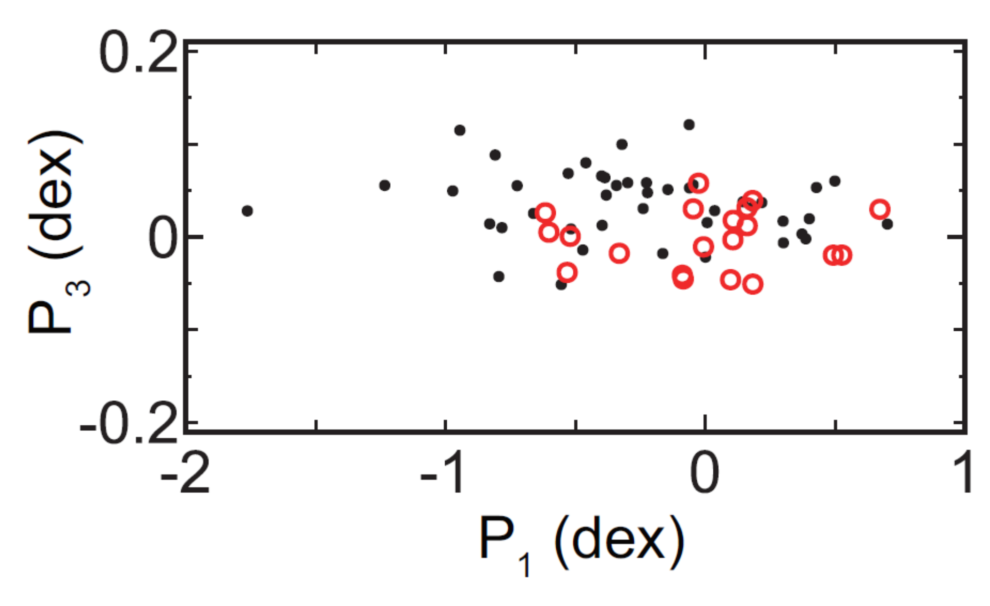

Black: XFP
Red: CFP

Fujita et al. (2018b)

▶ Plane shift

- Systematic difference of r_s and M_s between XFP and CFP can be estimated from the shift of the two FPs

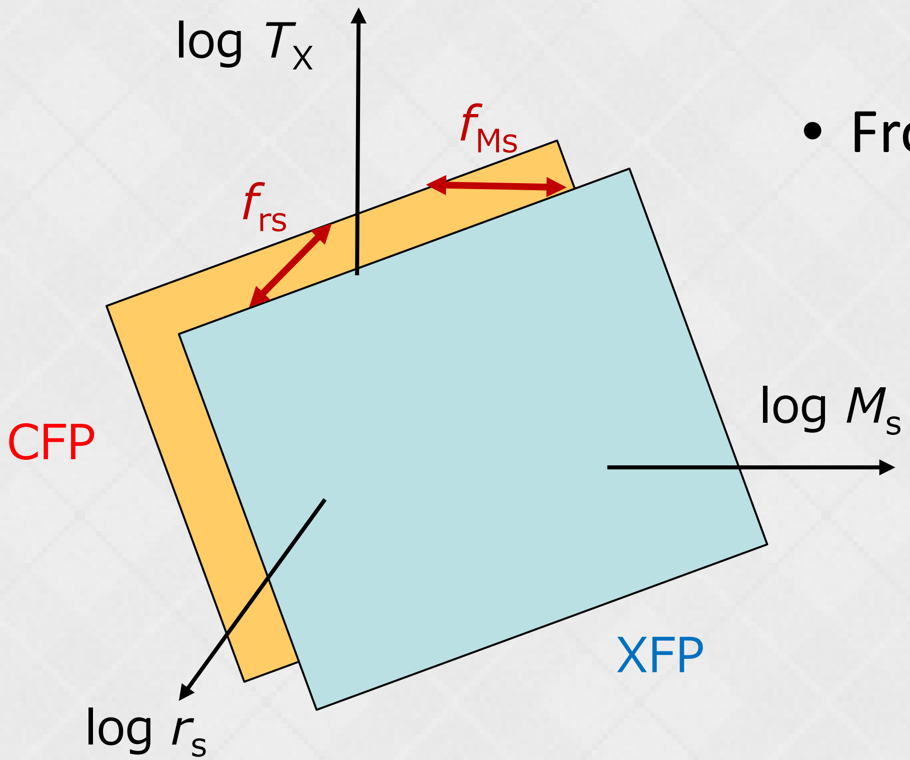

- From the observations of the FPs

$$f_{Ms} = M_{sX}/M_{sC} \sim 0.9$$

$$f_{rs} = r_{sX}/r_{sC} \sim 1.1$$

▶ Mass difference

- Assuming the NFW profile, f_{Ms} and f_{rs} can be analytically converted to mass bias $f_{M\Delta}$ = $M_{\Delta X}/M_{\Delta C}$ as a function of $C_{\Delta X}$ or $C_{\Delta C}$
  - $M_{\Delta X}$: M_{Δ} for XFP (M_{Δ} measured in X-rays; hydrostatic mass)
  - $M_{\Delta C}$: M_{Δ} for CFP (M_{Δ} measured by Grav. lensing; lensing mass)
    - Δ = 200, 500, etc
  - $C_{\Delta X}$: concentration parameter for XFP
  - $C_{\Delta C}$: concentration parameter for CFP

Mass difference

- $f_{M\Delta} = M_{\Delta X}/M_{\Delta C}$

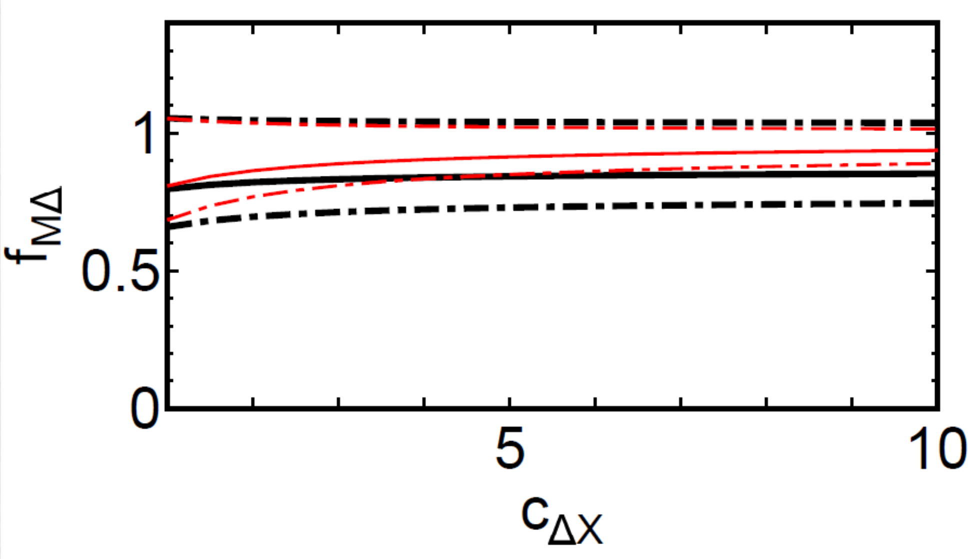

Mass bias estimated from the shift of the XFP and CFP

Fujita et al. (2018b)

- $f_{M\Delta}$ does not much depend on c_Δ
  - $f_{M\Delta} \sim 0.85 \pm 0.2$
    - X-ray (hydrostatic) mass tends to be smaller than Grav. lensing mass
    - Larger samples will allow us to determine $f_{M\Delta}$ more precisely

Summary

- Clusters form a fundamental plane (FP) in the space of ($\log r_s$, $\log M_s$, $\log T_X$)
  - T_X is determined by the formation time like r_s and M_s
- Clusters are growing and not in simplified virial equilibrium
  - Initial collapse and subsequent accretion should be considered separately

Summary

- Mass-temperature relation of clusters can be explained by the FP and the mass dependence of the concentration parameter
- Baseline L_X-T_X relation must be shallower
- FP can be used for mass calibration